Author/s:
Schienstock, D;Mueller, SN

Title:
Moving beyond velocity: Opportunities and challenges to quantify immune cell behavior*

Date:
2022-03-01

Citation:
Schienstock, D. & Mueller, S. N. (2022). Moving beyond velocity: Opportunities and challenges to quantify immune cell behavior*. Immunological Reviews, 306 (1), pp.123-136. https://doi.org/10.1111/imr.13038.

DR SCOTT N. MUELLER (Orcid ID : 0000-0002-3838-3989)

Article type : Invited Review

# Moving beyond velocity: Opportunities and challenges to quantify immune cell behavior

Dominik Schienstock,[1] and Scott N. Mueller[1,*]

[1]Department of Microbiology and Immunology, The University of Melbourne, The Peter Doherty Institute for Infection and Immunity, Melbourne, Australia.

*Correspondence:
Scott Mueller, Department of Microbiology and Immunology, The University of Melbourne, at The Peter Doherty Institute for Infection and Immunity, Melbourne 3000, Victoria, Australia. Email: smue@unimelb.edu.au

Funding information
This work was supported by grants from the National Health and Medical Research Council of Australia and the Australian Research Council (DP190103691)

Conflict of interest
The authors have no conflicts of interest to declare.

Data availability statement
Data sharing not applicable – no new was generated.

**Summary**

The analysis of cellular behavior using intravital multi-photon microscopy has contributed substantially to our understanding of the priming and effector phases of immune responses. Yet, many questions remain unanswered and unexplored. Though advancements in intravital imaging techniques and animal models continue to drive new discoveries, continued improvements in analysis methods are needed to extract detailed information about cellular behavior. Focusing on dendritic cell (DC) and T cell interactions as an exemplar, here we discuss key limitations for intravital imaging studies and review and explore alternative approaches to quantify immune cell behavior. We touch upon current developments in deep learning models, as well as established methods from unrelated fields such as ecology to detect and track objects over time. As developments in open-source software make it possible to process and interactively view larger datasets, the challenge for the field will be to determine how best to combine intravital imaging with multi-parameter imaging of larger tissue regions to discover new facets of leukocyte dynamics and how these contribute to immune responses.

Keywords:

Multi-photon microscopy, T cell migration, cell motility, image analysis, cell tracking

## 1 INTRODUCTION

Intravital microscopy is a technique that is used to image cells and tissues within living animals in order to capture cellular movement and observe biological processes. This method has greatly expanded knowledge previously obtained from *in vitro* observations. In the field of immunology, T cell behavior and interactions with antigen presenting cells (APCs) is one area where intravital microscopy has greatly expanded understanding of physiological cellular interactions (1-3). T cell activation and subsequent differentiation is facilitated by the formation of tight immunological synapses with APCs presenting cognate antigens. *In vitro* experiments to study T cell activation have the advantage to control factors that influence cell-cell interactions, including T cell or APC density, antigen dose, cytokine or growth factor availability, etc. However, these conditions might be different in an *in vivo* setting and transpire in the context of complex microanatomical niches where tissue cells and other immune cells provide many soluble and cell-associated signals that influence cell behavior. Although *in vitro* conditions provide the means to more readily interrogate cell signaling and

biochemical pathways, *in vivo* imaging can uncover cell behaviors that may not occur in the reductionist conditions present *in vitro* or even *ex vivo* in isolated tissues.

Leukocytes are highly motile cells that readily respond to environmental changes in order to protect the body. T cells follow paths of least resistance during their migration while they propel themselves forward by a contracting uropod (4). T cells in particular can adopt vastly different cell shapes and motility patterns as part of cell migration programs that facilitate diverse behaviors such as the search of cognate antigen in LNs (5) and immunosurveillance of peripheral tissues (6). These different behaviors are defined by soluble signals as well as interactions with the mechanical environment (4, 7). We recently examined how physiological neural signals influence immune cell behavior. T cells were found to stop migration following activation of the sympathetic nervous system or in response adrenergic receptor agonists (8). Loss of cell motility had a detrimental effect on immune responses to viral infections and tumor development. These experiments highlight that alterations to cell behavior can have marked impacts on the effectiveness of immune responses. Therefore, observing T cell behavior *in situ* is an exceptional way to explore and interrogate physiological cell behavior. The challenge however is to extract meaningful biological information from complex intravital imaging data.

In this review, we discuss the requirements and limitations of using intravital imaging to interrogate immune responses and advances in available methods to analyze and quantitate cell behavior. We use T cell priming by dendritic cells (DCs) in lymph nodes (LNs) as an instructive example of complex cellular behaviors that can be imaged by intravital microscopy. These lessons might however be used to interrogate immune responses in various other contexts of homeostasis or disease.

## 2 TRACKING CELLULAR INTERACTIONS DURING T CELL PRIMING IN LYMPH NODES

Interactions between T cells and DCs that lead to T cell activation and differentiation involve recognition of peptide-major histocompatibility complexes (pMHC). In a seminal study, Mempel et al. (9) observed a sequential sequence of T cell behavior during priming and activation. Initially, T cells undergo brief interactions with APCs that resemble transient pauses in motility. This scanning behavior was proposed to facilitate initial activation through summation of signals from multiple APCs (9). Upon stable recognition of an APC presenting cognate antigen, T cells cease motility and form an immunological synapse to gather activation signals for a period lasting up to several hours. Subsequently, T cells disengage,

regain motility and undergo proliferation and differentiation, during which time cells may receive additional antigen signals from other APCs (10).

Several studies have demonstrated the requirement of conventional DCs (cDCs) for effective T cell priming and differentiation of memory cells. cDC1s express the chemokine receptor XCR1 and C-type lectin-like receptor Clec9a and are specialized for cross-presentation of antigens for presentation on MHC-I and activation of $CD8^+$ T cells (11-13). cDC2s on the other hand have been shown to play key roles in the priming of $CD4^+$ T cells (5, 14). Lymphoid organs contain resident cDCs that develop locally from precursors and do not leave the tissue. Conversely, DCs that develop in the tissues migrate to LNs via the lymphatic vessels, both in the steady state and at increased rates in response to inflammation. These migratory DCs can be infected in the tissues or acquire antigens from the tissue and present these to T cells in LNs after their arrival. In some cases, pathogens can also drain directly to LNs via the lymphatics, or enter the spleen from the blood, and infect lymphoid organ resident DCs. Antigen-bearing migratory DCs can also transfer antigens to LN resident cDC1s upon their arrival in LNs (15). Together, these networks of resident and migratory cDCs in LNs, and resident DCs in the spleen, provide ample opportunities for antigen presentation to T cells to initiate immune responses.

Precisely how T cells acquire activation signals from subtypes of cDCs has yet to be fully elucidated. We previously defined the sequence of temporally and spatially segregated $CD4^+$ T helper and $CD8^+$ T killer cell activation in the LN following skin HSV infection (5). $CD4^+$ T cells initially clustered with skin-emigrant antigen bearing DCs while $CD8^+$ T cells clustered subsequently with $XCR1^+$ cDC1s. A similar sequence of events was observed following Vaccinia virus infection, with the distinction that direct infection of draining LN DCs enabled early $CD8^+$ T cell priming in this model (16), as opposed to delayed $CD8^+$ T cell priming following skin HSV infection due to lack of direct viral drainage to LNs (5). Following activation, $CD4^+$ T cells were frequently observed to "visit" $CD8^+$ T cell-DC clusters (5), suggesting that these activated $CD4^+$ T cells provide key helper signals to DCs through CD40-CD40L and CD70-CD27 signals (17). Yet, definitive proof that $CD4^+$ T cells deliver help signals in this manner, or via other interactions with cDC1s, is currently lacking.

In the studies described above (5, 16), and in other studies, T cell activation was inferred from visualization of T cell clustering with DCs (18-20). T cell activation may however also occur in the absence of tight immunological synapses. Dynamic interactions between T cells and APCs that do not involve T cell arrest, termed kinapses, have been proposed to facilitate progressive accumulation of activation signals from multiple APCs (21-

24). Recently activated T cells were shown to engage in kinapses with APCs *in vivo*, whereas naïve T cells formed stable synapses (21). Both transient and stable interactions between T cells and APCs presenting different pMHC complexes has also been demonstrated (25). Whether immunological kinapses play a role in naïve T cell priming in natural settings of infection or anti-tumor immunity remains unclear. Nevertheless, several signals can alter the duration of T-APC interactions. A high amount of antigen can induce the rapid induction of stable T-APC interactions, effectively bypassing an initial phase of transient interactions (25). Conversely, low levels of antigen induce initial T cell activation without stable T-APC interactions (26). Similarly, low-affinity TCR-pMHC interactions result in shorter duration interactions with APCs (27). Adhesion molecules, such as ICAM-1 expression by DCs (28) promote T-DC interactions. Co-inhibitory molecules including programmed death 1 (PD-1) and CTLA-4, and $CD4^+$ T regulatory cells (Tregs) reduce stable interactions with APCs (29-32). Therefore, T-APC interactions of various types and durations together contribute to T cell activation and influence the differentiation of T cells into effector and memory cell fates.

Significant technical challenges exist to track and quantitate the full spectrum of cellular interactions that comprise the phases of T cell priming *in vivo*. To follow the accumulation of activation signals by T cells, genetically encoded fluorescent reporters that accumulate over time could be used. TCR signaling in response to strong interaction with pMHC complexes involves rapid changes in intracellular calcium concentration in T cells (33, 34). Ulbricht et al. (35) recently developed a genetic fluorescence resonance energy transfer (FRET) construct with the calcium sensor Troponin C (Tnc) and eCFP and Citrine as donor and acceptor molecules, respectively. Binding of calcium to Tnc will trigger FRET transfer from eCFP to Citrine. The advantage of this system, compared to other calcium reporters (36-38) is that it is possible to quantify the accumulation of calcium signals over time. This was used to follow the development of B cells during germinal center reactions (35). Calcium concentrations could be linked to antigen specific responses but also to transient and stable contacts of B cells with follicular dendritic cells and subcapsular sinus macrophages within the LN. Such an approach might also allow insight into signal integration in T cells over time.

Quantifying calcium signals and detecting peaks of calcium activity is not trivial. Immune cells will move in and out of the imaging plane and increase or decrease in signal intensity due to differences in tissue scattering and depth. Related studies interrogating interactions between autoreactive Th17 cells and regulatory T cells activity in the context of experimental autoimmune encephalomyelitis (EAE) utilized a tandem calcium reporter with

tdTomato and GCaMP6f to quantify the ratio between both cytoplasmic fluorophores (38, 39). In a related study, Kryatsous et al. (40) used the FRET-based calcium sensor Twitch1 in combination with NFAT-GFP to measure not only calcium signaling but also subsequently T cell activation by translocation of NFAT to the nucleus. One caveat in intravital two-photon studies is that only 4 – 5 colours can be imaged simultaneously. It is therefore difficult to discern interactions of T cell subtypes with different APC subtypes. Hor et al. (5) utilized a combination of the XCR1-venus reporter mice and the skin-painting dye Tetramethylrhodamine (TRITC) to label migrating DCs. In this way it was possible to distinguish two APC subtypes and their specific interactions with $CD4^+$ and $CD8^+$ T cells (15).

To identify more complex interactions between immune cells subtypes with two-photon imaging, a combination of reporters in necessary. Ruhland et al. (41) interrogated which APC subtypes were able to acquire antigenic material from a subcutaneously injected tumor cell line using intravital imaging. The authors utilized a fluorescent genetic construct, ZsGreen, in B16-F10 melanoma cells to first confirm material transfer using flow cytometry and *in vitro* imaging. Catching these transfer events using intravital imaging is inherently difficult as they might be rare and hard to spot. A combination of three reporter lines, XCR1-venus, CD11c-mCherry and CSF1R-CFP, were used to distinguish between multiple DC and monocyte subsets and observed antigen transfer between these subsets *in vivo*. These studies highlight the importance of cell interactions between multiple different cell types to augment responses. Therefore, as we discuss further below, it is important to keep in mind that interactions and exchanges between cells that we are currently unaware of might have a significant impact on immune responses. These interactions might however not be directly obvious to the human observer and might be "hidden" by more prominent patterns in cell behaviors.

In addition to improved methods to image these events, better methods to extract meaningful information from imaging data might provide novel insights into the cellular interactions that drive immune responses. In the remainder of this review, we will focus on the factors that influence and determine which quantitative measures can be applied when quantifying immune cell behavior from intravital imaging data.

## 3 LIMITATIONS FOR QUANTITATIVE MEASUREMENTS OF INTRAVITAL IMAGING DATA

While intravital microscopy is a powerful tool to identify and discover immune cell behavior, there are significant limitations that need to be considered when planning and conducting intravital imaging studies. We discuss some of the main limitations and considerations, using the sequence of cellular interactions that occur in LNs during the priming of T cell responses as an example.

**3.1 Imaging depth.**

The capacity to image beyond the superficial surface of tissues is a significant limiting factor when using intravital microscopy. We can only observe cellular behavior in areas that are accessible via multi-photon excitation. Two-photon excitation involves the use of fast (usually femtosecond) pulses of intense long wavelength light that enables almost simultaneous delivery at the point of focus of two photons of half the power required to excite a fluorescent protein. The use of longer wavelengths of light reduces light scattering, allowing deeper tissue penetration and can produce less photo-damage to tissues. Imaging depth is limited by the degree of light absorption and scattering by different tissues and increasing laser power leads to increased out-of-focus fluorescence and damage through heating of the tissues.

In LNs, two-photon imaging of interactions beyond 250-300 μm beneath the capsule are very difficult to achieve. This precludes imaging into the depth of the T cell zone where much of the activation and priming events will take place. T cell migration in the lymph is dependent on complex chemokine gradients (42). naïve T cells are retained in the T cell area by CCL19/CCL21 where they can interact with DCs. Upon activation, $CD4^+$ T cells downregulate CCR7 and upregulate CXCR5 to migrate to the T-B border to interact with B cells (42). These initial events within the T cell zone are precluded from observation by intravital imaging. Duckworth et al. (43) recently utilized lightsheet imaging to interrogate the effect of chemokine gradients and T cell position during T cell differentiation into short lived effector and memory T cells. T cells differentiated in the periphery and paracortex of the LN while the initial activation and priming is occurring deep in the medullary region where the T cell zone resides. With two-photon microscopy we are only able to see these peripheral events. To image the medullary regions of LNs, researchers have used successfully images explanted tissues (44), but access to these regions *in vivo* remains challenging. This challenge is also faced by researchers analyzing T cell behavior in other lymphoid organs, such as the spleen. Chauveau et al. (45) used intravital imaging to investigate migration patterns of lymphocytes from the red pulp to the white pulp via bridging channels. The

authors used a combination a several analysis methods to quantify the flow of cells close to blood vessels within bridging channels of wildtype and CCR7$^{-/-}$ mice. CCR7 was found to be important for the directional movement of T cells to the T cell zone via bridging channels; yet, insights into cell behaviors in the depth of the T cell zone remain obscured.

Depth limitations for intravital imaging might be overcome by technical advances in imaging modalities, including three-photon excitation and adaptive optics. Three-photon microscopy has been utilized in the field of neuroscience to gain insights into neuronal communications in the brain, including imaging over 1 mm into the cortex in mice (46-48). The slow repetition rate of three-photon lasers and high power required to achieve coincident excitation pose unique challenges for intravital imaging of rapidly moving immune cells. Yet, three-photon microscopy has the potential to uncover yet unseen and unknown T cell behavior deep within secondary lymphoid tissues as well as in other tissues.

Adaptive optics is an approach that attempts to utilize advances in the field of astronomy to reduce the impact of the refractory index mismatch by adaptive mirrors. To correct for light aberrations introduced by the tissues and improve the resolution of imaging, deformable mirrors and wavefront sensors can be used. These mirrors must be tightly controlled by associated software components to achieve the desired distortion corrections. The technique was proposed some time ago to image deeper tissue regions (49). Adaptive optics techniques have been applied to deep in vivo imaging, for instance enabling imaging up to 700 μm in the brain (50). Adaptive optics was recently applied to large scale imaging of various organs due to advances in microscopy and computational tools (51). Other approaches have used video rate raster scanning combined with adaptive optics to improve image quality (52). As both adaptive optics and three-photon approaches improve, we expect to see greatly improved intravital imaging at depths in tissues that are currently out of reach.

**3.2 Imaging volume.**

The choice of imaging volume will influence what kind of data, analysis and conclusions can be drawn from imaging studies. We frequently image T cells in the LNs with an imaging volume of around 60 μm and a time interval of 30 – 45 sec (5). An alternative is to capture a smaller imaging volume at a higher imaging frequency (53). Intravital imaging of more dynamic events, such as imaging of calcium signaling, requires a more rapid imaging frequency (i.e. 5 – 15 fps), reducing the volume of tissue that can be imaged unless more rapid scanning is achieved, such as using resonant or rotating polygonal scanners. Smaller imaging volumes are more prone to errors resulting from axial tissue drift. The choice of

these parameters depends on the goal of the subsequent quantification and analysis. To make sensible conclusions of parameters such as velocity and angle, a certain amount of granularity is required. When these dynamic measurements are not the primary focus and positioning over a bigger area is more important, the imaging area can be increased and imaging frequency decreased. Advances in widefield (54) and two-photon (55, 56) lightsheet fluorescent microscopes could alleviate some of the mentioned limitations. Lightsheet systems apply a sheet of light, instead of scanning with a single localized beam, as in confocal and multi-photon imaging. The advantage is a gain in acquisition speed, but often a reduction in resolution. Lightsheet microscopy is frequently used in developmental biology to image the development of whole embryos, for example from the fruit fly *Drosophila melanogaster*, over time (57). For more rapid intravital imaging, an exciting alternative to lightsheet imaging is to use reverberation microscopy, whereby simultaneous beams are produced that can scan at increasing depths simultaneously (58).

**3.3 Imaging time**.

The sequence of cellular interactions that occur in LNs during the priming of T cell responses have largely been extrapolated from short periods of intravital imaging lasting approximately 1-2 hours. Therefore, with current technologies, researchers are unable to follow the extended life of a T cell across the time period of days during which full effector differentiation occurs. This is due both to limitations in imaging time and the capacity to follow cells through the extended volume of the tissue (in this case, the LNs). Restrictions on how long an animal can remain anesthetized in combination with a limited depth and field of view limit current intravital imaging capacity. To extract robust information, data from different animals are typically compared in order to build a coherent picture of immune responses over time. Thus, results may be heavily dependent on how robust the experimental model is. To make more precise conclusions over time, approaches have been developed to image the same mouse over time. Examples include surgically implanted imaging windows for LNs (59), the brain (60) and tumors (61). Recently, imaging windows have even been used to image the developing mouse embryo over time (62). The advantage of this method is that immune responses and disease progression can be followed in a specific mouse over time.

**3.4 Fluorescent reporters.**

Genetically encoded fluorescent reporters and cell dyes generally need to be very bright to facilitate efficient excitation and fluorescence in deep tissues. Timpson and colleagues (63)

recently reviewed many available genetic reporters for intravital imaging and different imaging modalities. T cells have long been shown to round up, decrease motility and increase calcium signaling upon interactions with antigen presenting cells (64, 65). Recently, Bohineust et. al. (33) showed that rounding up and stopping could be specifically induced *in vivo* by triggering calcium signaling with optogenetic tools. Calcium signaling is however only a transient event and might only be captured within one frame during intravital imaging. Reporters that indicate T cell activation, for example via NFAT translocation (66), have been developed for two photon imaging studies.

These reporters however only report on signaling within single cells. The context must be inferred from interacting cells which might be labelled differently, or unlabeled, and unable to report the signaling event. An alternative strategy is to specifically label interactions between specified cell types. A system termed 'Labelling Immune Partnerships by SorTagging Intercellular Contacts' (LIPSTIC) was utilized to visualize T helper cell signaling via CD40 with cognate APCs (67). The system depends on a tag consisting of five N-terminal glycine residues (G5) that was linked to CD40 on the APC and an enzyme, sortase A, which is linked to CD40L on the $CD4^+$ T cell. During interactions, a fluorescent or biotin tagged peptide sequence is supplied which is recognized and processed by sortase A and transferred to the acceptor molecule G5. Using this system, Pasqual et al. (67) demonstrated labelling of "helped" DCs *in vivo* by using antigen loaded. These tools could be used to discover early priming in the immune response and the delivery of helper signals but have yet to be visualized by intravital imaging.

## 4 APPROACHES FOR QUANTIFYING IMMUNE CELL BEHAVIOR

Given the challenges and limitations in acquiring high temporal and spatial resolution intravital imaging data, appropriate analysis of the resulting data is essential to obtain reliable biological information. Studies in ecology have encountered similar limitations and challenges albeit on a different scale. GPS data from tracked animals is often sparse and can only give a certain amount of detail (68). Caution is necessary when interpreting cell motility parameters such as velocity, angle and directionality. These measurements are dependent on the total time an object is being tracked, the time interval between images and the accuracy of the tracking analysis. Many studies have used velocity and angle to quantify T cell migration patterns (1, 8, 9, 19, 69-71). These measurements were important to elucidate the behavior patterns observed in the initial T cell priming and effector stages (*Figure 1a*). But to extract additional behavior patterns that are more subtle may require the integration of different

measures. To appropriately analyze intravital imaging movies, several steps should be considered and the choice at each step will influence the resulting quantification. Imaris (Bitplane) is a common choice of image analysis software for many immunologists working with intravital imaging data. This is an excellent, albeit costly, option with the advantage of ease of use for image processing and filtering to object detection, tracking and segmentation. Below, we discuss open-source software alternatives and highlight the opportunities that these tools and approaches might have for customization of image analysis.

**4.1 Object detection and tracking.**

T cells can assume various shapes depending on the biochemical and mechanical properties of the tissue (4). Cells can be amoeboid when migrating, spherical when sessile or display varying degrees of dendriticity when probing their environment. These changes occur frequently, and the difficulty is to detect these cells as objects and produce a valid segmentation. Given the wide choice of tools to segment objects in images, the decision process to identify the best tool for the job depends heavily on the characteristics of the images and the objects (cells) within these (*Figure 2*, *Table 1*).

Many processing routines for live cell imaging depend on detection of blob-like objects. A common approach is to compute the Laplacian of Gaussian (72), which detects edges, with subsequent maxima detection. This process requires the definition of a radius to detect objects of interest. A radius too high can lead to over-detection while a radius too low will result in under-detection. Migrating T cells might be split into two objects while sessile T cells might be merged into one object because of inaccurate object detection. For many image analysis workflows this is the default choice. The advantage is that it can be utilized on relatively noisy or dim images many of the settings can be adjusted by the user. A different approach was recently proposed by developers of the ImageJ plugin Trackmate (73, 74). Their tracking algorithms now allow the input from deep learning (DL) segmentation algorithms such as StarDist (75, 76) and Cellpose (77).

DL is a type of machine learning (ML). ML and DL algorithms take annotated images for training and attempt to predict objects in unseen datasets. The main difference between the two is that DL can process unstructured data whereas data must be pre-processed for ML. DL algorithms such as StarDist and Cellpose utilize neural networks that attempt to simulate the functioning of the brain. The advantage of these is that they can be specifically trained to detect nuclei-like (StarDist and Cellpose) or cell-like (Cellpose) objects. Cellpose was developed as a generalist cell segmentation algorithm (77); that means, it was trained on a

plethora of images that look like nuclei or cells – even unrelated images such as sea shells were utilized. The result is a framework that can provide segmentation in 2D and 3D with pre-trained models which can approximate the diverse shapes of T cells. These segmentation results can be utilized by Trackmate for further downstream processing.

Once objects are identified within images or image sequences these need to be tracked. T cells migrate via undirected random walks (78), and display substantial considerable heterogeneity in speed and turning angles (79). The tracking analysis of cells can be performed using software such as Imaris, or with tools such as Trackmate (73, 74). Trackmate primarily uses a process termed the linear assignment problem (LAP) to following migrating cells (73, 80). LAP links objects in consecutive frames which are subsequently combined into full tracks by a global optimization algorithm (80). The user sets the search radius in which the algorithm will link objects together and how many missing frames will be allowed to link objects across frames. These values are dependent on how fast and far T cells will migrate in the specific imaging volume. An alternative approach, bTrack (81), uses a Kalman filter to learn and predict future object positions, and a Bayesian believe matrix to assign probabilities that objects belong to a track or will start a new track. The authors of this method utilized this python framework to track cell cycle progression *in vitro* of the mammalian cell line Madin-Darby Canine Kidney cells (MDCK) (81). The efficacy of this approach for tracking highly motile cells *in vivo* is untested.

A combination of sessile and migrating T cells in the same space can be problematic for tracking as migrating T cell tracks will be mixed up with sessile T cell track when they are in close proximity. Such track switches might be overcome by considering more information than just cell positioning. The field of pedestrian tracking is utilizing DL approaches to detect and track objects over time using all information from the images (82, 83). One could envision that these multi-object tracking algorithms could be utilized for T cell tracking to make use of all the available information, including cell shape and volume, to reduce the number of tracking errors and manual user corrections required.

### 4.2 Following the path of migrating cells.

Cell tracks, or the measurable path that migrating cells are observed to take within the imaging volume, are often relatively short, lasting only a few minutes as T cells move in and out of the imaging plane. The track length should be taken into account when quantifying cellular behavior. When large numbers of rapidly moving fluorescent cells are present in the imaging volume, cell tracking software algorithms are often unable to follow individual cell

paths, frequently losing track of cells or misinterpreting cell tracks for cells that pass or interact with each other as mentioned above. Devi et al. (8) analyzed changes in T cell behavior in response to neural signaling in the LN. Automated cell tracking was used to determine the instantaneous velocity of cells over time. This was useful to define when cells ceased migration due to reduction in oxygen levels. By comparison, when individual cell tracking is challenging and longer duration tracks are required to infer cell behavior, this method might not be the best choice. Gerard et al. (84) attempted to overcome this limitation by simulating longer duration tracks from multiple shorter tracks. While useful in certain scenarios, the approach of simulating cell behavior may not reveal unexpected cell behaviors that depend on parameters that are not included in the computational model.

To quantify T cell migration within the bridging channels of the spleen during intravital imaging (45), a computational approach, MOtion SEnsing Superpixels (MOSES) was employed (85). MOSES is a combination of single cell tracking and particle image velocimetry (PIV), which estimates the velocity of pixels within a given window (85). The algorithm utilizes superpixels which groups similar local pixels together. Using this method, the user can extract single cell tracks and the flow of cells within crowded environments. The impact of short track lengths on the inference of cell movement was reduced in this example (45). Limitations in track length might therefore not be a problem. This enabled the researchers to estimate "flow" patterns of T cells in the spleen through the bridging channels to the T cell zone. Crowded cells are also frequently observed when T cells are primed in the LN (5) which makes commonly used tracking approaches less reliable.

Alternative approaches to deal with track length limitations involve unitization of tracks into 'tracklets' and focusing on individual cell states rather than the whole tracks. Pizzagalli et al. (86) chose to split tracks into 'tracklets' of a defined length of 500 s using a sliding window approach. The resulting 'tracklets' were analyzed using conventional track statistics to extract neutrophil behavior patterns during influenza vaccination. This categorization is however only dependent on the given time window. T cells frequently change behavior over the course of a track, which is not always the same length in time. Arts et al. (87) proposed a new classification of tracks into distinct behavioral 'tracklets' using DL. DL need training data in order to predict unseen data. The authors simulated tracks to train the DL model to detect fast, slow and immobile objects and showcased this method on different datasets of protein mobility (87).

A different approach to classify track segments into behavior patterns is to utilize hidden markov models (HMMs) (88). HMMs attempt to identify different modes of behavior

in a given timeseries (*Figure 1d*). This technique is often utilized in ecological research to extract patterns of animal behavior (89). An advantage of this approach is that the state of any object only depends on the preceding image or timepoint. This is both a strength and a limitation of this approach because it does not account for the history of the cell or object. This approach was used to identify transcriptional bursts of estrogen-responsive gene *TFF1* within the human breast cancer cell line MCF7 cells using single-molecule imaging (90). HMM is a relatively simple method and has several implementations in most scripting languages; yet, has, to our knowledge, so far not been utilized analyze intravital imaging movies.

**4.3 Cell behavior characteristics.**

Various track statistics are commonly calculated from intravital imaging data and used to classify and extract different cellular behavior patterns (91) (*Figure 3*, *Table 2*). Trackmate provides several track measurements such as meandering index, mean velocity and mean angle (73). The resulting tracks are often subsequently analyzed with custom MATLAB or R scripts commonly used by statisticians. To facilitate this process and extract more information from tracking measurements, Wortel et al. (92) developed an R package termed CelltrackR. This package combines several 'standard' tracking measurements but also extends this analysis to classify these tracks into distinct categories and create simulations of the observed datasets.

In general, tracks can be classified into classes based on velocity, displacement, meandering index or confinement ratio (net displacement / total distance travelled) and arrest coefficient (fraction of time cells spend with a velocity less than a defined value, often 2 μm/min for T cells) (*Figure 1b*, *c*). T cell behavior can be classified into four different categories: directed (high velocity, high meandering index), confined (low velocity, low meandering index), returning (low velocity, high meandering index), and stop-and-go (low velocity, high meandering index) (20, 38). Sivapatham et al. (93) used a combination of these measurements to analyze T cell behavior during the first 72 h after infection of high and low load of LCMV Clone 13 footpad injection. Intravital imaging of the popliteal LN showed that LCMV specific $CD4^+$ and $CD8^+$ T cells decreased in speed and meandering index and arrested only modestly with a low viral load. A higher viral load increased scanning behavior by T cells. This reductionist system was able to visualize synapse-like behavior with different levels of antigen present. These types of interactions are harder to analyze in settings such as infection where the antigen load and the subtypes of DCs presenting antigen cannot be

controlled (5). Under these conditions, relatively simple measurements might not be sufficient to extract subtle changes in cell behavior.

Nonetheless, Pizzagalli et al. (86) identified five different modes of neutrophil behavior during influenza vaccination using a combination of the arrest coefficient, straightness, displacement, velocity, proximity to blood vessels and clustering of cells: flowing inside blood vessels, arresting (high arrest coefficient), patrolling (non-arrested but confined), directed (high speed and displacement) and swarming (clustering cells). However, the threshold used to define arresting cells is subjective and can be difficult to define. For this reason, Pizzagalli, Latino (86) used a sigmoidal thresholding function to determine the arrest coefficient to reduce fluctuations (86). Conversely, a HMM could be utilized to classify different modes of behavior by identifying states from the data itself rather than from a set manual threshold (89).

While HMMs are theoretically useful, they might require more information than velocity and angle from a single stained cell population (94). Given the vast availability of cellular reporters for intravital imaging (63) it will be important to measure general cellular properties such as the shape of the cell, the intracellular actin cytoskeleton, the cell membrane, the nucleus or calcium signaling. This was useful for the CellProfiler community to measure many different cellular parameters in high throughput imaging studies to study the effect of different drug combinations, termed cell-painting (95). Hons et al. (96) utilized a combination of intravital imaging of the pLN and *in vitro* microscopy to quantify actin flow, using Lifeact-GFP mice, and membrane / lipid dynamics, using a synthetic dye, during T cell migration in the LN. The authors focused on T cells that moved horizontally in the imaging view to analyze shape and behavior in 2D, which is markedly easier than 3D. Continuous actin flow from the leading to the trailing edge was visualized using fluorescence recovery after photobleaching (FRAP). These cellular parameters could be used in HMMs to uncover more contextual information about immune cell behavior and interactions with other cells in the tissue microenvironment.

Lau et al. (71) utilized similar measures in combination with T cell shape to highlight behavior patterns during tumor development – inside and outside the tumor. T cells have a directed and stop-and-go behavior outside the tumor while their motility gets more and more confined as they approach into the tumor. Within the tumor, T cells were highly confined and killed their target by adopting a more rounded shape compared to an ellipsoid migratory shape – akin to the synapse formation between DCs and T cells.

Most approaches use 'gating' of track statistics to classify behavior. Methods such as dynamic time warping (DTW), which are used, for example, in speech recognition and ecology to classify words and sound or motility patterns could theoretically be applied to cell motility (88, 97). DTW is a measurement to quantify the similarity between two time-series patterns which can vary in length. A T cell might show migrating behavior, then slow down and regain motility again; this pattern could occur faster or slower, but the pattern is similar (*Figure 1e*). This method has so far not been utilized to classify cellular tracks. T cells show highly motile and switching behavior even within single tracks. This method might therefore be difficult to apply to whole tracks; yet, classifying shorter tracklets with this algorithm is tempting and might achieve a similar informative classification as described above by Arts et al. (87) who used DL methods to classify tracklets.

Inspiration for methods to track the dynamic movement of immune cells can be drawn from ecology, where animal movement patterns have been studies. For example, the analysis of *Argyrodes elevates,* a foraging spider that invades other's spider's webs in search of food (98), has many similar analysis metrices. The authors used DTW to classify the trajectories of *A. elevates* invading other spider nests and quantified revisits to the web with the R package 'recurse' (99). The invading spider used a circling behavior with high motility at the periphery of the web and slower motility while repeatedly visiting sites close to the main hub. This behavior is like T cells which migrate with a high velocity and slow down when encountering a DC or a T cell cluster which they might revisit repeatedly (38). A caveat for intravital imaging studies is that cells leaving the imaging volume entirely before returning would not be recognized as repeat visitors unless some form of cell labelling was used, such as genetically-encoded photomodulatable proteins including KikGR or photoactivatable GFP (100, 101).

**4.4 Cell-cell interactions.**

Direct cellular contact and clustering of T cells with APCs has been frequently used as a surrogate for T cell activation events (5, 19, 20). Upon contact with DCs, T cells received activation signals which can be visualized by calcium signaling (33, 64) (*Figure 1f*). Identifying and accurately tracking clustering T cells is inherently difficult, which is where DL algorithms might helpful, as discussed earlier. Furthermore, as cells move and occasionally coalesce, a cluster might only form for a very brief period. A cluster detection algorithm may not be able to correctly identify these transient behaviors. There are several approaches to tackle this. In R the 'runmed' function from the 'stats' package will run an

overlapping median across the whole timeseries. Therefore, outliers will be removed. The same principle can also be used to cleanup noisy velocity and angle measurements, whereby small movements of the sample or errors in tracking introduce cell movement artefacts. These artefacts can be filtered to reduce fluctuations in the signal. Fluctuations in the signal can be problematic when using classification algorithms, such as HMM or DTW, as these outliers might be classified together.

Motile cells undergo frequent interactions with other cells in the tissue microenvironment, including other lymphocytes, DCs and macrophages, fibroblastic and endothelial stromal cells. Many of these cells are not fluorescently labelled during typical intravital imaging experiments and are therefore effectively invisible. For example, cDCs are the major cell population that presents antigens to T cells for priming, but other cells including B cells, macrophages, and stromal cells can also present antigens to T cells. Although these APCs present fewer pMHC complexes or lack costimulatory molecules, these might cumulatively contribute to the magnitude or quality of the resulting T cell responses. To understand how T cells acquire signals from multiple APCs during the process of activation, inferring cell interactions from analysis of cell behavior in combination with specific reporters of cell signaling could allow recognition of such 'invisible' interactions. Cells might show a specific behavior that could be picked up by classifying tracklets with DL or DTW, or using HMM to detect individual cell states.

### 4.5 Mapping immune cell behavior to tissue environment

A major limitation of many imaging approaches is the capacity to capture a sufficient number of colors to detect multiple cell types and cell states simultaneously. This is particularly true for intravital multi-photon microscopy. However, several methods that enable multi-parameter staining and imaging of fixed samples have substantially improved spatial analysis of cell locations and cellular phenotypes. One such approach is histo-cytometry (102-104), which involves segmentation in Imaris (Bitplane), subsequent flow cytometry gating in FlowJo (FlowJo LLC) and exporting defined populations into the MATLAB application CytoMAP (102) to extract regions of similar cellular composition. This approach has been used highly effectively to map the cellular environment in static images (102-104). Using flow cytometry methods to gate on cellular tracks has also been used to analyze two-photon microscopy data (24). In both static and dynamic images, regions can be defined in various ways and used for further analysis such as clustering and dimensionality reduction and neighborhood analysis. To achieve this, the image can be tiled into overlapping squares or

tiles or individual cells can be used to define individual regions within a defined circle (2D) or sphere (3D) around them (102).

Applying this principle of regions to the study of dynamic cell behavior could involve the extraction and definition of individual cell behavior over time in different areas. Although we previously observed T cell clustering during T cell activation using two photon imaging and then mapped clustering over a larger region of the tissue area (5), directly linking *in vivo* cell behavior to cell phenotypes is more challenging. The goal would be to acquire live imaging data from a small imaging volume using a limited number of colors, followed by isolation and fixation of the tissue and acquisition of static images using a larger number of markers to identify cell types. This could be used to match cell behavior to cell phenotypes. This approach will require methods such as photomodulatable or photoactivatable proteins to tag cells or tissue niches for subsequent identification of the same region by static imaging. It is worth noting that this approach has been used successfully to profile cells by single cell RNA sequencing after live imaging (105, 106).

More studies linking dynamic T cell behavior with static image analysis are required to push the field forward. To achieve this and make these approaches more accessible, the learning curve of applying these methods has to be flattened. Current methods and software for analysis of imaging data separate the tracking and downstream plotting and analysis steps, for example by first processing images in Imaris (Bitplane) and/or ImageJ and subsequent data display or analysis using Prism, Python, MATLAB and/or R. This disconnect between image processing and analysis makes it harder to visualize downstream analysis and makes the learning curve to analyze images for researchers unfamiliar with these scripting very steep.

One solution could integrate interactive analysis with visualization on the original image. Tools for tracking, analysis and plotting and visualizing data on images are available in R, Python, and MATLAB (*Table 3*). This will help to identify cell behaviors while not losing contact to the original image. Some efforts have been taken into this direction (107-109) and we would encourage researchers to explore various options to make alternative analysis methods more accessible. The popularity of a multidimensional image viewer in Python, napari (napari.org), has recently grown and actively supported by the image analysis community (forum.image.sc/tag/napari). Dynamic plotting and user interactions can be implemented relatively simple in Python's Dash (plotly.com/dash/) and R's Shiny package (shiny.rstudio.com). The image analysis community is also in the process of defining a cloud-based image file format, termed Next-Generation File Format (NGFF) (110), based on the

chunked multidimensional Zarr file format (zarr.readthedocs.io/en/stable/). This file format enables efficient writing and reading of larger datasets and would provide a file format that is shaped by the image analysis for the needs of the end-users. That means, user can have an influence on how images are stored, how segmentation is stored, how tracking data and respective analysis is stored and how applications will be able to interact with this format.

## CONCLUSION

Intravital multi-photon imaging has provided an in-depth view of immune cell behavior *in situ*. It has highlighted the scope of the dynamic cellular interactions required for immune responses to occur and to be sustained. As technological advances enable imaging deeper into tissues, it is an imperative to use all available information form these images to uncover and understand the complexities of cell behavior. Here, we introduced some of the possible approaches and opportunities that could be used to improve analysis of immune cell dynamics and learn from these behavior patterns to reveal the intricacies of life at the cellular level.

**FIGURE 1:** Analysis of T cell behavior during priming and effector phases. a) Different modes of cellular behavior are observed as T cells progress through priming and effector phases. b) Typical track measurements taken by studies are primarily based on velocity and angle. Confined cells mostly stay in a specific area with lower motility. Directed motion shows relatively high velocity and lower angle. Returning cells show a relatively high velocity while being more confined to one larger area. Turning points are identified by a sharp decrease in speed and increase in angle. Stop-and-go motion is defined by a cell scanning with intermittent higher velocity – cells are overall slow in motility but reach further in their migration. c) These different kinds of behavior can be identified by plotting mean velocity, meandering index (net distance / total distance), displacement and arrest coefficient (fraction of track with a velocity less than 2 μm/min). d) Hidden markov model (HMM) to identify underlying behavior from observed behavior. e) Dynamic time warping (DTW) to identify tracks with similar motility patterns. f) Calcium reporters can be used in combination with velocity and contact with other cells to infer T cell activation.

**FIGURE 2:** A decision tree for image segmentation. Clean and bright (high signal to noise) images can be segmented with deep learning (DL) or machine learning (ML) methods. These methods can yield better segmentation compared to classic seed-based approaches. Seed-based image segmentation approaches however can be used to extract quantitative information even from noisy or dim (low signal to noise) images. Relevant applications and packages are listed in *Table 1*.

**FIGURE 3:** A decision tree to create tracks and conduct relevant analysis from intravital imaging data. If cells are not too crowded and their behavior is relatively stable over the imaging period, the extraction of common tracking statistics will in most cases be sufficient. If cells are too crowded, tracking of cells can be challenging and alternative methods, such superpixel tracking can be utilised. If cells are frequently changing their behavior during the imaging period, tracklets or a Hidden markov model (HMM) can be utilised to extract more biologically meaningful behavior. Relevant applications and packages are listed in *Table 2*.

## REFERENCES


1. Bousso P. T-cell activation by dendritic cells in the lymph node: lessons from the movies. Nat Rev Immunol. 2008;8(9):675-84.
2. Germain RN, Jenkins MK. In vivo antigen presentation. Curr Opin Immunol. 2004;16(1):120-5.
3. Ugur M, Mueller SN. T cell and dendritic cell interactions in lymphoid organs: More than just being in the right place at the right time. Immunol Rev. 2019;289(1):115-28.
4. Lammermann T, Germain RN. The multiple faces of leukocyte interstitial migration. Semin Immunopathol. 2014;36(2):227-51.
5. Hor JL, Whitney PG, Zaid A, Brooks AG, Heath WR, Mueller SN. Spatiotemporally Distinct Interactions with Dendritic Cell Subsets Facilitates CD4+ and CD8+ T Cell Activation to Localized Viral Infection. Immunity. 2015;43(3):554-65.
6. Gebhardt T, Whitney PG, Zaid A, Mackay LK, Brooks AG, Heath WR, et al. Different patterns of peripheral migration by memory CD4+ and CD8+ T cells. Nature. 2011;477(7363):216-9.
7. Lammermann T, Kastenmuller W. Concepts of GPCR-controlled navigation in the immune system. Immunol Rev. 2019;289(1):205-31.

8. Devi S, Alexandre YO, Loi JK, Gillis R, Ghazanfari N, Creed SJ, et al. Adrenergic regulation of the vasculature impairs leukocyte interstitial migration and suppresses immune responses. Immunity. 2021;54(6):1219-30 e7.
9. Mempel TR, Henrickson SE, Von Andrian UH. T-cell priming by dendritic cells in lymph nodes occurs in three distinct phases. Nature. 2004;427(6970):154-9.
10. Celli S, Garcia Z, Bousso P. CD4 T cells integrate signals delivered during successive DC encounters in vivo. J Exp Med. 2005;202(9):1271-8.
11. Giza HM, Bozzacco L. Unboxing dendritic cells: Tales of multi-faceted biology and function. Immunology. 2021.
12. Gutierrez-Martinez E, Planes R, Anselmi G, Reynolds M, Menezes S, Adiko AC, et al. Cross-Presentation of Cell-Associated Antigens by MHC Class I in Dendritic Cell Subsets. Front Immunol. 2015;6:363.
13. Merad M, Sathe P, Helft J, Miller J, Mortha A. The dendritic cell lineage: ontogeny and function of dendritic cells and their subsets in the steady state and the inflamed setting. Annu Rev Immunol. 2013;31:563-604.
14. Eisenbarth SC. Dendritic cell subsets in T cell programming: location dictates function. Nat Rev Immunol. 2019;19(2):89-103.
15. Allan RS, Waithman J, Bedoui S, Jones CM, Villadangos JA, Zhan Y, et al. Migratory dendritic cells transfer antigen to a lymph node-resident dendritic cell population for efficient CTL priming. Immunity. 2006;25(1):153-62.
16. Eickhoff S, Brewitz A, Gerner MY, Klauschen F, Komander K, Hemmi H, et al. Robust Anti-viral Immunity Requires Multiple Distinct T Cell-Dendritic Cell Interactions. Cell. 2015;162(6):1322-37.
17. Feau S, Garcia Z, Arens R, Yagita H, Borst J, Schoenberger SP. The CD4(+) T-cell help signal is transmitted from APC to CD8(+) T-cells via CD27-CD70 interactions. Nat Commun. 2012;3:948.
18. Baptista AP, Gola A, Huang Y, Milanez-Almeida P, Torabi-Parizi P, Urban JF, Jr., et al. The Chemoattractant Receptor Ebi2 Drives Intranodal Naive CD4(+) T Cell Peripheralization to Promote Effective Adaptive Immunity. Immunity. 2019;50(5):1188-201 e6.
19. Bousso P, Robey E. Dynamics of CD8+ T cell priming by dendritic cells in intact lymph nodes. Nat Immunol. 2003;4(6):579-85.

20. De Giovanni M, Cutillo V, Giladi A, Sala E, Maganuco CG, Medaglia C, et al. Spatiotemporal regulation of type I interferon expression determines the antiviral polarization of CD4(+) T cells. Nat Immunol. 2020;21(3):321-30.
21. Azar GA, Lemaitre F, Robey EA, Bousso P. Subcellular dynamics of T cell immunological synapses and kinapses in lymph nodes. Proc Natl Acad Sci U S A. 2010;107(8):3675-80.
22. Dustin ML. Hunter to gatherer and back: immunological synapses and kinapses as variations on the theme of amoeboid locomotion. Annu Rev Cell Dev Biol. 2008;24:577-96.
23. Moreau HD, Bousso P. Visualizing how T cells collect activation signals in vivo. Curr Opin Immunol. 2014;26:56-62.
24. Moreau HD, Lemaitre F, Terriac E, Azar G, Piel M, Lennon-Dumenil AM, et al. Dynamic in situ cytometry uncovers T cell receptor signaling during immunological synapses and kinapses in vivo. Immunity. 2012;37(2):351-63.
25. Henrickson SE, Mempel TR, Mazo IB, Liu B, Artyomov MN, Zheng H, et al. T cell sensing of antigen dose governs interactive behavior with dendritic cells and sets a threshold for T cell activation. Nat Immunol. 2008;9(3):282-91.
26. Henrickson SE, Perro M, Loughhead SM, Senman B, Stutte S, Quigley M, et al. Antigen availability determines CD8(+) T cell-dendritic cell interaction kinetics and memory fate decisions. Immunity. 2013;39(3):496-507.
27. Ozga AJ, Moalli F, Abe J, Swoger J, Sharpe J, Zehn D, et al. pMHC affinity controls duration of CD8+ T cell-DC interactions and imprints timing of effector differentiation versus expansion. J Exp Med. 2016;213(12):2811-29.
28. Scholer A, Hugues S, Boissonnas A, Fetler L, Amigorena S. Intercellular adhesion molecule-1-dependent stable interactions between T cells and dendritic cells determine CD8+ T cell memory. Immunity. 2008;28(2):258-70.
29. Fife BT, Pauken KE, Eagar TN, Obu T, Wu J, Tang Q, et al. Interactions between PD-1 and PD-L1 promote tolerance by blocking the TCR-induced stop signal. Nat Immunol. 2009;10(11):1185-92.
30. Schneider H, Downey J, Smith A, Zinselmeyer BH, Rush C, Brewer JM, et al. Reversal of the TCR stop signal by CTLA-4. Science. 2006;313(5795):1972-5.
31. Tadokoro CE, Shakhar G, Shen S, Ding Y, Lino AC, Maraver A, et al. Regulatory T cells inhibit stable contacts between CD4+ T cells and dendritic cells in vivo. J Exp Med. 2006;203(3):505-11.

32. Tang Q, Adams JY, Tooley AJ, Bi M, Fife BT, Serra P, et al. Visualizing regulatory T cell control of autoimmune responses in nonobese diabetic mice. Nat Immunol. 2006;7(1):83-92.
33. Bohineust A, Garcia Z, Corre B, Lemaitre F, Bousso P. Optogenetic manipulation of calcium signals in single T cells in vivo. Nat Commun. 2020;11(1):1143.
34. Skokos D, Shakhar G, Varma R, Waite JC, Cameron TO, Lindquist RL, et al. Peptide-MHC potency governs dynamic interactions between T cells and dendritic cells in lymph nodes. Nat Immunol. 2007;8(8):835-44.
35. Ulbricht C, Leben R, Rakhymzhan A, Kirchhoff F, Nitschke L, Radbruch H, et al. Intravital quantification reveals dynamic calcium concentration changes across B cell differentiation stages. Elife. 2021;10.
36. Chen TW, Wardill TJ, Sun Y, Pulver SR, Renninger SL, Baohan A, et al. Ultrasensitive fluorescent proteins for imaging neuronal activity. Nature. 2013;499(7458):295-300.
37. Dong TX, Othy S, Greenberg ML, Jairaman A, Akunwafo C, Leverrier S, et al. Intermittent Ca(2+) signals mediated by Orai1 regulate basal T cell motility. Elife. 2017;6.
38. Othy S, Jairaman A, Dynes JL, Dong TX, Tune C, Yeromin AV, et al. Regulatory T cells suppress Th17 cell Ca(2+) signaling in the spinal cord during murine autoimmune neuroinflammation. Proc Natl Acad Sci U S A. 2020;117(33):20088-99.
39. Jairaman A, Othy S, Dynes JL, Yeromin AV, Zavala A, Greenberg ML, et al. Piezo1 channels restrain regulatory T cells but are dispensable for effector CD4(+) T cell responses. Sci Adv. 2021;7(28).
40. Kyratsous NI, Bauer IJ, Zhang G, Pesic M, Bartholomaus I, Mues M, et al. Visualizing context-dependent calcium signaling in encephalitogenic T cells in vivo by two-photon microscopy. Proc Natl Acad Sci U S A. 2017;114(31):E6381-E9.
41. Ruhland MK, Roberts EW, Cai E, Mujal AM, Marchuk K, Beppler C, et al. Visualizing Synaptic Transfer of Tumor Antigens among Dendritic Cells. Cancer Cell. 2020;37(6):786-99 e5.
42. Stein JV, Nombela-Arrieta C. Chemokine control of lymphocyte trafficking: a general overview. Immunology. 2005;116(1):1-12.
43. Duckworth BC, Lafouresse F, Wimmer VC, Broomfield BJ, Dalit L, Alexandre YO, et al. Effector and stem-like memory cell fates are imprinted in distinct lymph node niches directed by CXCR3 ligands. Nat Immunol. 2021;22(4):434-48.

44. Grigorova IL, Schwab SR, Phan TG, Pham TH, Okada T, Cyster JG. Cortical sinus probing, S1P1-dependent entry and flow-based capture of egressing T cells. Nat Immunol. 2009;10(1):58-65.
45. Chauveau A, Pirgova G, Cheng HW, De Martin A, Zhou FY, Wideman S, et al. Visualization of T Cell Migration in the Spleen Reveals a Network of Perivascular Pathways that Guide Entry into T Zones. Immunity. 2020;52(5):794-807 e7.
46. Hontani Y, Xia F, Xu C. Multicolor three-photon fluorescence imaging with single-wavelength excitation deep in mouse brain. Sci Adv. 2021;7(12).
47. Ouzounov DG, Wang T, Wang M, Feng DD, Horton NG, Cruz-Hernandez JC, et al. In vivo three-photon imaging of activity of GCaMP6-labeled neurons deep in intact mouse brain. Nat Methods. 2017;14(4):388-90.
48. Yildirim M, Sugihara H, So PTC, Sur M. Functional imaging of visual cortical layers and subplate in awake mice with optimized three-photon microscopy. Nat Commun. 2019;10(1):177.
49. Tao X, Fernandez B, Azucena O, Fu M, Garcia D, Zuo Y, et al. Adaptive optics confocal microscopy using direct wavefront sensing. Opt Lett. 2011;36(7):1062-4.
50. Wang K, Sun W, Richie CT, Harvey BK, Betzig E, Ji N. Direct wavefront sensing for high-resolution in vivo imaging in scattering tissue. Nat Commun. 2015;6:7276.
51. Wu J, Lu Z, Jiang D, Guo Y, Qiao H, Zhang Y, et al. Iterative tomography with digital adaptive optics permits hour-long intravital observation of 3D subcellular dynamics at millisecond scale. Cell. 2021;184(12):3318-32 e17.
52. Li Y, Lim YJ, Xu Q, Beattie L, Gardiner EE, Gaus K, et al., editors. Raster Adaptive Optics for Video Rate Laser Scanning Microscopy with Large Field of View Correction. Conference on Lasers and Electro-Optics; 2020 2020/05/10; Washington, DC: Optical Society of America.
53. Sammicheli S, Kuka M, Iannacone M. Intravital Imaging of B Cell Responses in Lymph Nodes. Methods Mol Biol. 2018;1763:63-74.
54. Takanezawa S, Saitou T, Imamura T. Wide field light-sheet microscopy with lens-axicon controlled two-photon Bessel beam illumination. Nat Commun. 2021;12(1):2979.
55. Truong TV, Supatto W, Koos DS, Choi JM, Fraser SE. Deep and fast live imaging with two-photon scanned light-sheet microscopy. Nat Methods. 2011;8(9):757-60.
56. Piksarv P, Marti D, Le T, Unterhuber A, Forbes LH, Andrews MR, et al. Integrated single- and two-photon light sheet microscopy using accelerating beams. Sci Rep. 2017;7(1):1435.

57. Tomer R, Khairy K, Amat F, Keller PJ. Quantitative high-speed imaging of entire developing embryos with simultaneous multiview light-sheet microscopy. Nat Methods. 2012;9(7):755-63.
58. Beaulieu DR, Davison IG, Kilic K, Bifano TG, Mertz J. Simultaneous multiplane imaging with reverberation two-photon microscopy. Nat Methods. 2020;17(3):283-6.
59. Meijer EFJ, Jeong HS, Pereira ER, Ruggieri TA, Blatter C, Vakoc BJ, et al. Murine chronic lymph node window for longitudinal intravital lymph node imaging. Nat Protoc. 2017;12(8):1513-20.
60. Cramer SW, Carter RE, Aronson JD, Kodandaramaiah SB, Ebner TJ, Chen CC. Through the looking glass: A review of cranial window technology for optical access to the brain. J Neurosci Methods. 2021;354:109100.
61. Wyckoff J, Gligorijevic B, Entenberg D, Segall J, Condeelis J. High-resolution multiphoton imaging of tumors in vivo. Cold Spring Harb Protoc. 2011;2011(10):1167-84.
62. Huang Q, Cohen MA, Alsina FC, Devlin G, Garrett A, McKey J, et al. Intravital imaging of mouse embryos. Science. 2020;368(6487):181-6.
63. Murphy KJ, Reed DA, Trpceski M, Herrmann D, Timpson P. Quantifying and visualising the nuances of cellular dynamics in vivo using intravital imaging. Curr Opin Cell Biol. 2021;72:41-53.
64. Donnadieu E, Bismuth G, Trautmann A. Antigen recognition by helper T cells elicits a sequence of distinct changes of their shape and intracellular calcium. Curr Biol. 1994;4(7):584-95.
65. Bhakta NR, Oh DY, Lewis RS. Calcium oscillations regulate thymocyte motility during positive selection in the three-dimensional thymic environment. Nat Immunol. 2005;6(2):143-51.
66. Pesic M, Bartholomaus I, Kyratsous NI, Heissmeyer V, Wekerle H, Kawakami N. 2-photon imaging of phagocyte-mediated T cell activation in the CNS. J Clin Invest. 2013;123(3):1192-201.
67. Pasqual G, Chudnovskiy A, Tas JMJ, Agudelo M, Schweitzer LD, Cui A, et al. Monitoring T cell-dendritic cell interactions in vivo by intercellular enzymatic labelling. Nature. 2018;553(7689):496-500.
68. Demsar U, Buchin K, Cagnacci F, Safi K, Speckmann B, Van de Weghe N, et al. Analysis and visualisation of movement: an interdisciplinary review. Mov Ecol. 2015;3(1):5.
69. Bousso P, Bhakta NR, Lewis RS, Robey E. Dynamics of thymocyte-stromal cell interactions visualized by two-photon microscopy. Science. 2002;296(5574):1876-80.

70. Larochelle C, Wasser B, Jamann H, Loffel JT, Cui QL, Tastet O, et al. Pro-inflammatory T helper 17 directly harms oligodendrocytes in neuroinflammation. Proc Natl Acad Sci U S A. 2021;118(34).

71. Lau D, Garcon F, Chandra A, Lechermann LM, Aloj L, Chilvers ER, et al. Intravital Imaging of Adoptive T-Cell Morphology, Mobility and Trafficking Following Immune Checkpoint Inhibition in a Mouse Melanoma Model. Front Immunol. 2020;11:1514.

72. Marr D, Hildreth E. Theory of edge detection. Proc R Soc Lond B Biol Sci. 1980;207(1167):187-217.

73. Tinevez JY, Perry N, Schindelin J, Hoopes GM, Reynolds GD, Laplantine E, et al. TrackMate: An open and extensible platform for single-particle tracking. Methods. 2017;115:80-90.

74. Ershov D, Phan M-S, Pylvänäinen JW, Rigaud SU, Le Blanc L, Charles-Orszag A, et al. Bringing TrackMate in the era of machine-learning and deep-learning. bioRxiv. 2021:2021.09.03.458852.

75. Schmidt U, Weigert M, Broaddus C, Myers G, editors. Cell Detection with Star-Convex Polygons2018; Cham: Springer International Publishing.

76. Weigert M, Schmidt U, Haase R, Sugawara K, Myers G. Star-convex Polyhedra for 3D Object Detection and Segmentation in Microscopy. Ieee Wint Conf Appl. 2020:3655-62.

77. Stringer C, Wang T, Michaelos M, Pachitariu M. Cellpose: a generalist algorithm for cellular segmentation. Nat Methods. 2021;18(1):100-6.

78. Krummel MF, Bartumeus F, Gerard A. T cell migration, search strategies and mechanisms. Nat Rev Immunol. 2016;16(3):193-201.

79. Jerison ER, Quake SR. Heterogeneous T cell motility behaviors emerge from a coupling between speed and turning in vivo. Elife. 2020;9.

80. Jaqaman K, Loerke D, Mettlen M, Kuwata H, Grinstein S, Schmid SL, et al. Robust single-particle tracking in live-cell time-lapse sequences. Nat Methods. 2008;5(8):695-702.

81. Ulicna K, Vallardi G, Charras G, Lowe AR. Automated deep lineage tree analysis using a Bayesian single cell tracking approach. bioRxiv. 2020:2020.09.10.276980.

82. Brunetti A, Buongiorno D, Trotta GF, Bevilacqua V. Computer vision and deep learning techniques for pedestrian detection and tracking: A survey. Neurocomputing. 2018;300:17-33.

83. Xu YH, Sep A, Ban YT, Horaud R, Leal-Taixe L, Alameda-Pineda X. How To Train Your Deep Multi-Object Tracker. Proc Cvpr Ieee. 2020:6786-95.

84. Gerard A, Patino-Lopez G, Beemiller P, Nambiar R, Ben-Aissa K, Liu Y, et al. Detection of rare antigen-presenting cells through T cell-intrinsic meandering motility, mediated by Myo1g. Cell. 2014;158(3):492-505.

85. Zhou FY, Ruiz-Puig C, Owen RP, White MJ, Rittscher J, Lu X. Motion sensing superpixels (MOSES) is a systematic computational framework to quantify and discover cellular motion phenotypes. Elife. 2019;8.

86. Pizzagalli DU, Latino I, Pulfer A, Palomino-Segura M, Virgilio T, Farsakoglu Y, et al. Characterization of the Dynamic Behavior of Neutrophils Following Influenza Vaccination. Front Immunol. 2019;10:2621.

87. Arts M, Smal I, Paul MW, Wyman C, Meijering E. Particle Mobility Analysis Using Deep Learning and the Moment Scaling Spectrum. Sci Rep. 2019;9(1):17160.

88. Aghabozorgi S, Shirkhorshidi AS, Wah TY. Time-series clustering - A decade review. Inform Syst. 2015;53:16-38.

89. McClintock BT, Michelot T. momentuHMM: R package for generalized hidden Markov models of animal movement. Methods Ecol Evol. 2018;9(6):1518-30.

90. Rodriguez J, Ren G, Day CR, Zhao K, Chow CC, Larson DR. Intrinsic Dynamics of a Human Gene Reveal the Basis of Expression Heterogeneity. Cell. 2019;176(1-2):213-26 e18.

91. Meijering E, Dzyubachyk O, Smal I. Methods for cell and particle tracking. Methods Enzymol. 2012;504:183-200.

92. Wortel IMN, Liu AY, Dannenberg K, Berry JC, Miller MJ, Textor J. CelltrackR: An R package for fast and flexible analysis of immune cell migration data. ImmunoInformatics. 2021;1-2:100003.

93. Sivapatham S, Ficht X, Barreto de Albuquerque J, Page N, Merkler D, Stein JV. Initial Viral Inoculum Determines Kinapse-and Synapse-Like T Cell Motility in Reactive Lymph Nodes. Front Immunol. 2019;10:2086.

94. Buderman FE, Gingery TM, Diefenbach DR, Gigliotti LC, Begley-Miller D, McDill MM, et al. Caution is warranted when using animal space-use and movement to infer behavioral states. Mov Ecol. 2021;9(1):30.

95. Bray MA, Singh S, Han H, Davis CT, Borgeson B, Hartland C, et al. Cell Painting, a high-content image-based assay for morphological profiling using multiplexed fluorescent dyes. Nat Protoc. 2016;11(9):1757-74.

96. Hons M, Kopf A, Hauschild R, Leithner A, Gaertner F, Abe J, et al. Chemokines and integrins independently tune actin flow and substrate friction during intranodal migration of T cells. Nat Immunol. 2018;19(6):606-16.

97. Aghabozorgi S, Ying Wah T, Herawan T, Jalab HA, Shaygan MA, Jalali A. A hybrid algorithm for clustering of time series data based on affinity search technique. ScientificWorldJournal. 2014;2014:562194.
98. Rosales-Garcia R, Tapia-McClung H, Narendra A, Rao D. Many paths, one destination: mapping the movements of a kleptoparasitic spider on the host's web. J Comp Physiol A Neuroethol Sens Neural Behav Physiol. 2021;207(2):293-301.
99. Bracis C, Bildstein KL, Mueller T. Revisitation analysis uncovers spatio-temporal patterns in animal movement data. Ecography. 2018;41(11):1801-11.
100. Chudnovskiy A, Pasqual G, Victora GD. Studying interactions between dendritic cells and T cells in vivo. Curr Opin Immunol. 2019;58:24-30.
101. Suan D, Nguyen A, Moran I, Bourne K, Hermes JR, Arshi M, et al. T follicular helper cells have distinct modes of migration and molecular signatures in naive and memory immune responses. Immunity. 2015;42(4):704-18.
102. Stoltzfus CR, Filipek J, Gern BH, Olin BE, Leal JM, Wu Y, et al. CytoMAP: A Spatial Analysis Toolbox Reveals Features of Myeloid Cell Organization in Lymphoid Tissues. Cell Rep. 2020;31(3):107523.
103. Li W, Germain RN, Gerner MY. High-dimensional cell-level analysis of tissues with Ce3D multiplex volume imaging. Nat Protoc. 2019;14(6):1708-33.
104. Gerner MY, Kastenmuller W, Ifrim I, Kabat J, Germain RN. Histo-cytometry: a method for highly multiplex quantitative tissue imaging analysis applied to dendritic cell subset microanatomy in lymph nodes. Immunity. 2012;37(2):364-76.
105. Bost P, Giladi A, Liu Y, Bendjelal Y, Xu G, David E, et al. Host-Viral Infection Maps Reveal Signatures of Severe COVID-19 Patients. Cell. 2020;181(7):1475-88 e12.
106. Medaglia C, Giladi A, Stoler-Barak L, De Giovanni M, Salame TM, Biram A, et al. Spatial reconstruction of immune niches by combining photoactivatable reporters and scRNA-seq. Science. 2017;358(6370):1622-6.
107. Kotov DI, Pengo T, Mitchell JS, Gastinger MJ, Jenkins MK. Chrysalis: A New Method for High-Throughput Histo-Cytometry Analysis of Images and Movies. J Immunol. 2019;202(1):300-8.
108. Masuzzo P, Huyck L, Simiczyjew A, Ampe C, Martens L, Van Troys M. An end-to-end software solution for the analysis of high-throughput single-cell migration data. Sci Rep. 2017;7:42383.
109. Czech E, Aksoy BA, Aksoy P, Hammerbacher J. Cytokit: a single-cell analysis toolkit for high dimensional fluorescent microscopy imaging. BMC Bioinformatics. 2019;20(1):448.

110. Moore J, Allan C, Besson S, Burel J-M, Diel E, Gault D, et al. OME-NGFF: scalable format strategies for interoperable bioimaging data. bioRxiv. 2021:2021.03.31.437929.
111. Arganda-Carreras I, Kaynig V, Rueden C, Eliceiri KW, Schindelin J, Cardona A, et al. Trainable Weka Segmentation: a machine learning tool for microscopy pixel classification. Bioinformatics. 2017;33(15):2424-6.
112. Berg S, Kutra D, Kroeger T, Straehle CN, Kausler BX, Haubold C, et al. ilastik: interactive machine learning for (bio)image analysis. Nat Methods. 2019;16(12):1226-32.
113. Ollion J, Cochennec J, Loll F, Escude C, Boudier T. TANGO: a generic tool for high-throughput 3D image analysis for studying nuclear organization. Bioinformatics. 2013;29(14):1840-1.
114. Legland D, Arganda-Carreras I, Andrey P. MorphoLibJ: integrated library and plugins for mathematical morphology with ImageJ. Bioinformatics. 2016;32(22):3532-4.
115. Visser I, Speekenbrink M. depmixS4: An R Package for Hidden Markov Models. Journal of Statistical Software. 2010;36(7):1 - 21.
116. Hardle W, Steiger W. Algorithm AS 296: Optimal Median Smoothing. Journal of the Royal Statistical Society Series C (Applied Statistics). 1995;44(2):258-64.
117. Giorgino T. Computing and Visualizing Dynamic Time Warping Alignments in R: The dtw Package. Journal of Statistical Software. 2009;31(7):1 - 24.
118. Rocklin M. Dask: Parallel Computation with Blocked algorithms and Task Scheduling. In: Huff K, Bergstra J, editors. Proceedings of the 14th Python in Science Conference2015. p. 130-6.
119. Wolf FA, Angerer P, Theis FJ. SCANPY: large-scale single-cell gene expression data analysis. Genome Biol. 2018;19(1):15.
120. Sofroniew N, Lambert T, Evans K, Nunez-Iglesias J, Bokota G, Winston P, et al. napari/napari: 0.4.11. 2021.
121. Eling N, Damond N, Hoch T, Bodenmiller B. Cytomapper: an R/bioconductor package for visualisation of highly multiplexed imaging data. Bioinformatics. 2020.

Table 1: Principles and software packages that can be utilized to segment cells from intravital imaging data.

| Term / Principle | Description | Packages / Application | Ref |
|---|---|---|---|
| Generalist Deep Learning Model | Model trained on a variety of similar looking images to detect a wider range of objects; not limited to the objects that the model was trained on | Cellpose (Python): 2D/3D nuclei and cytoplasm segmentation | (77) |
| Specific Deep Learning Model | Model trained on specific images | StarDist (Python): 2D/3D nuclei segmentation | (75, 76) |
| Machine learning | User defined positive and negative pixels to train image segmentation algorithms | Trainable weka segmentation (ImageJ)<br>Ilastik | (111)<br>(112) |
| Seed detection | For example, by Laplacian of Gaussian (LoG) which is a gaussian filter (filters noise) with subsequent Laplacian filter (detects edges) and maxima detection for larger objects. Alternative for smaller objects, difference of two gaussian filters with subsequent Laplacian filter and maxima detection. | TrackMate (ImageJ) | (73) |
| Seed-based Watershed segmentation | Images treated as topographic map with pixel intensity as height to find ridges between adjacent objects | 3D ImageJ Suite (ImageJ) | (113) |
| Seed-based Spot segmentation | Determination of local threshold around seeds to classify surrounding pixels; Watershed segmentation is used to split objects | 3D ImageJ Suite (ImageJ) | (113) |
| Morphological filtering | Series of morphological filters to enhance object detection and segmentation by subsequent watershed operation | MorpholibJ (ImageJ) | (114) |

Table 2: Principles and software packages that can be utilized to track and analyse resulting cell tracks. For a comprehensive overview on tracking software and tracking statistics see Meijering et al. (91).

| **Term / Principle** | **Description** | **Packages / Application** | **Ref** |
|---|---|---|---|
| Displacement | Linear distance from the start to finish of track | TrackMate (ImageJ) with MATLAB; CelltrackR (R): Suite of various tracking measures and simulation abilities | (73, 92) |
| Meandering Index | Total displacement/path length of a cell track | | |
| Straight linear speed | Total displacement/Total time of a cell track | | |
| Instantaneous velocity | Speed of a cell at a specific point in time | | |
| Turning angle | Angle between two sequential points | | |
| Arrest Coefficient | Proportion of cells within a track with velocity < 2 - 4 μm/min | | |
| Revisitation sites | Identification of cells that visit a site, region or other cell more than once within one track | recurse (R) | (99) |
| Superpixel tracking | Pixels with similar intensities are grouped into superpixels resulting in cell tracking and estimation of the flow of cellular movement | MOSES (Python) | (85) |
| Tracklets | Splitting of tracks into segments with subsequent analysis | Overlapping sliding windows with defined length tracklets | (86) |
| | | Segments of behaviour patterns extracted by DL models | (87) |
| Hidden Markov Model (HMM) | Extraction of hidden states behind observed behavior | depmixS4 (R) | (115) |
| | | Classification of animal behaviour | (89) |
| Noise filtering | Noise from cell-based | runmean, runmed (R) | (116) |

| | | | |
|---|---|---|---|
| | statistics and classification can be filtered over time with, for example, running median or mean operations | | |
| Dynamic time warping (DTW) | Computation of local stretch and compression to detect segments that exhibit similar patterns over time | dtw (R / Python) | (117) |
| Clustering algorithms | Commonly used algorithms, for example Gaussian Mixture Models, can be used to classify tracks into distinct groups based on the calculated statistics | ClusterR (R) | https://CRAN.R-project.org/package=ClusterR |

Table 3: Software for storing and visualizing images and tracking data.

| Description | Package | Ref |
|---|---|---|
| Specification for next-generation file format File format (NGFF) to read and write large multidimensional images in cloud storage | OME-NGFF (Zarr / Python) | (110) |
| Framework to process large matrices in parallel processes | Dask Array (Python) | (118) |
| Hierarchical Data Format 5 (HDF5) based format to read and write single cell sequencing datasets which is also usable to manage cell and tracking statistics | Scanpy / Anndata (Python) | (119) |
| Interactive, multidimensional viewer to visualize static and live images | napari (Python) | (120) |
| Visualizing multidimensional data on images which could be utilized to plot tracking statistics on images | cytomapper (R) | (121) |

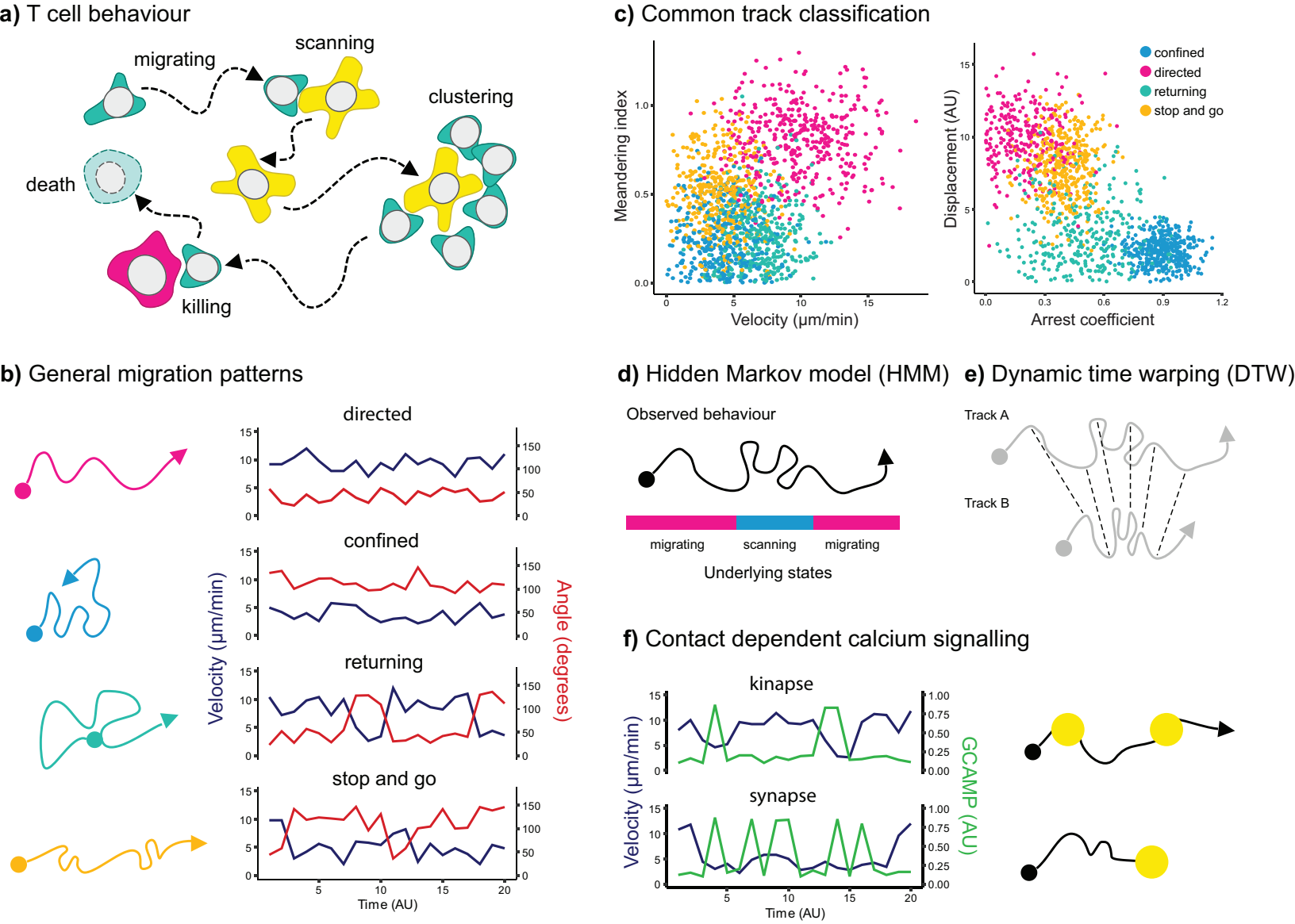


imr_13038_f1.eps

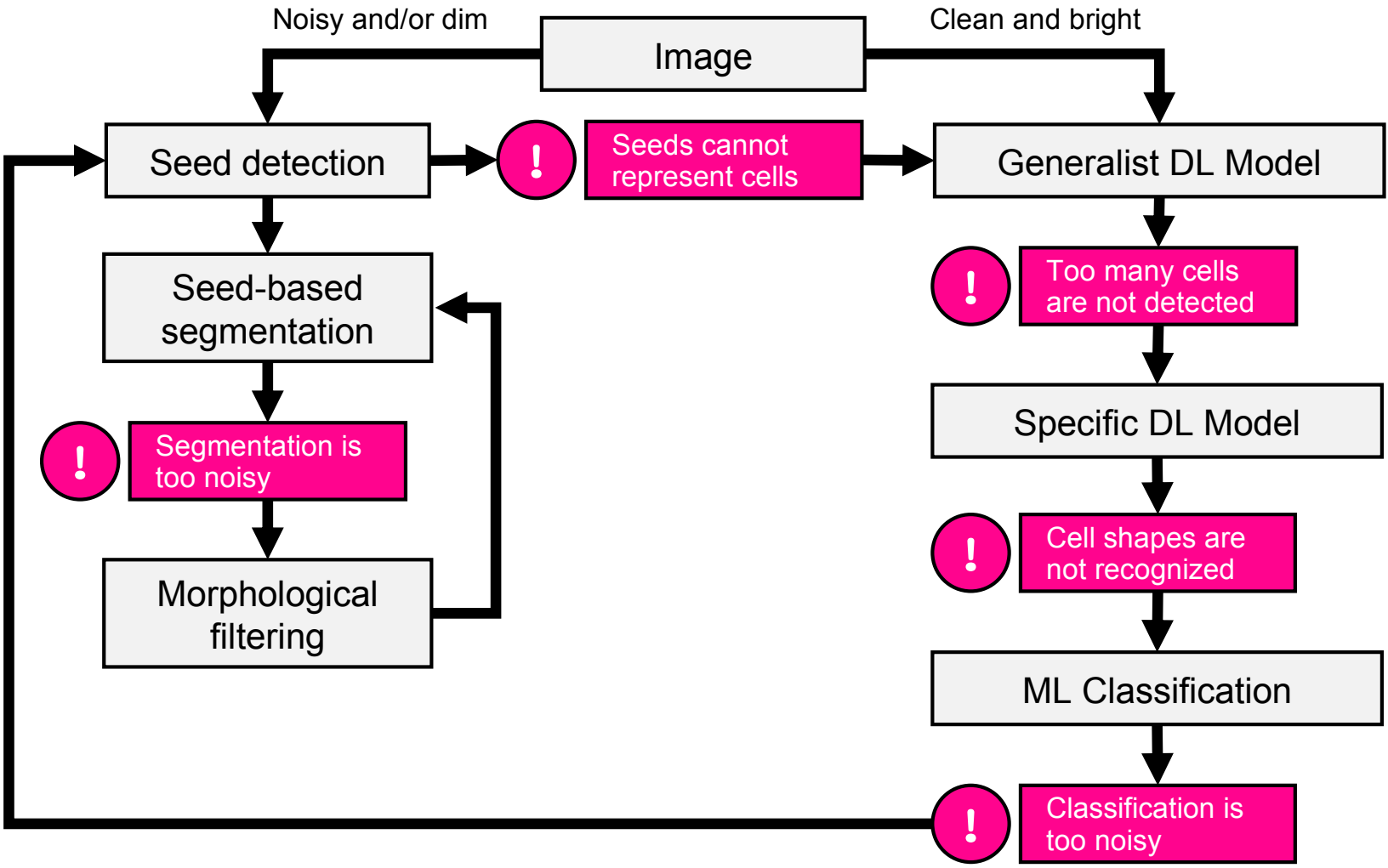


imr_13038_f2.eps

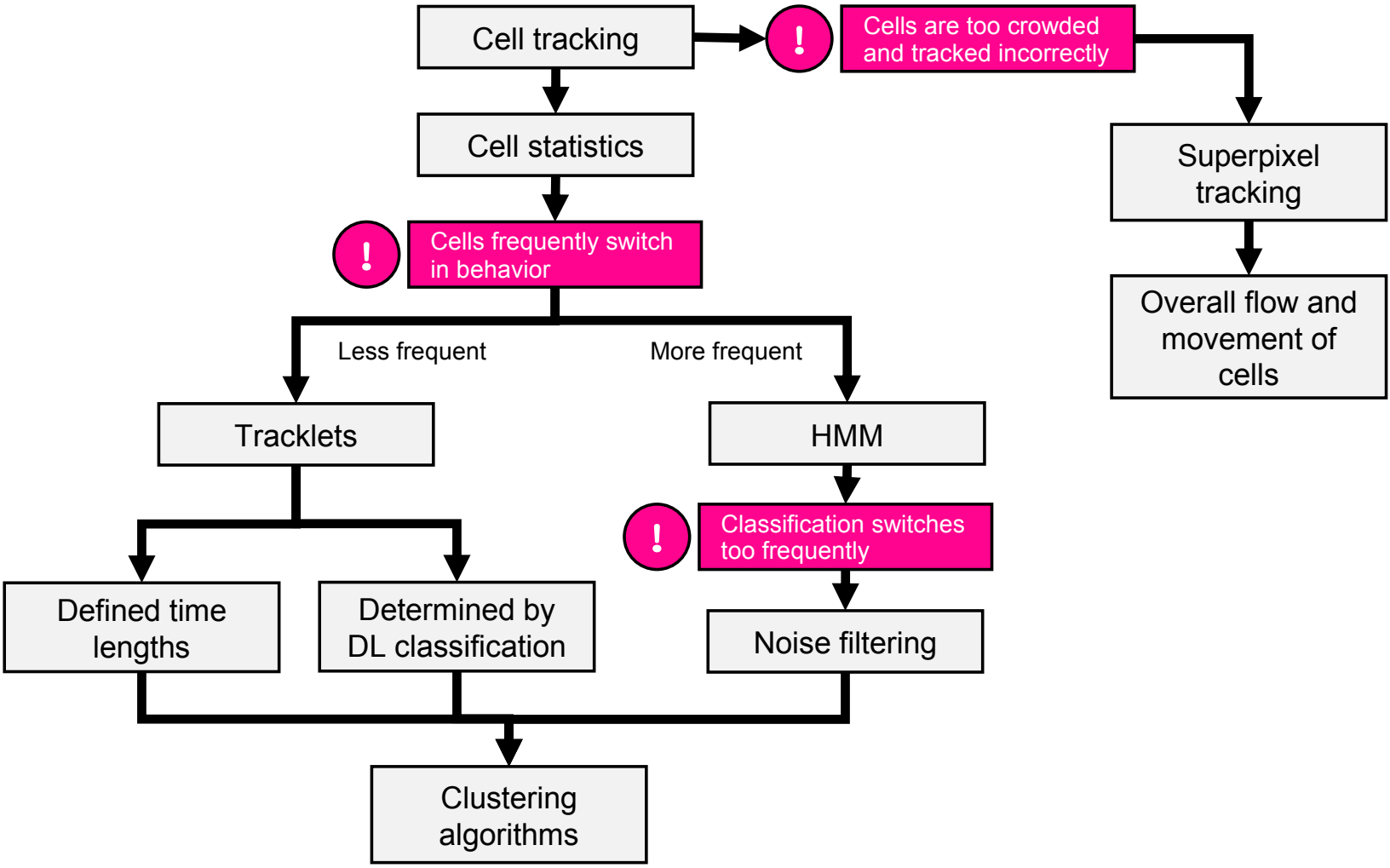


imr_13038_f3.eps